Optimal control of selective vibrational excitation in harmonic linear chain molecules

Shenghua Shi, Andrea Woody, and Herschel Rabitz
Department of Chemistry, Princeton University, Princeton, New Jersey 08544

(Received 27 October 1987; accepted 28 January 1988)

A formalism for designing an optical field for selective vibrational excitation in linear harmonic chain molecules is presented based on optimal control theory. The optimizing functional producing the field designs is flexible to allow for the imposition of desirable laboratory and theoretical constraints. The designed optimal fields, which successfully lead to local bond excitations, exhibit complex structure on the time scale of 10 fs. Analysis of the optimal fields shows a high degree of cooperativety between the temporal structure of the fields and the dynamical capabilities of the molecules. It is generally impossible using only spectral information to devise the optical field needed to selectively excite a local bond in a polyatomic molecule. These results explain why the previous intuitively based laboratory attempts at site specific chemistry have yielded disappointing results.

I. INTRODUCTION

The advent of lasers has generated great interest in selective excitation and bond-selective chemistry in polyatomic molecules. Unfortunately, the extensive theoretical and experimental studies stimulated by this interest seem to lead to the conclusion that, because of rapid intramolecular vibrational redistribution, laser induced selectivity is not, in general, feasible.[1–3] However, previous attempts have relied on spectral information of the isolated molecules and basically applied physical intuition to choose the laser pumping sources. The previous studies, thus, seem only to suggest that the selectivity can not be achieved by simple guessing at the nature of the optical field. But the desired goal might still be realizable if one takes into account the details of the system dynamics in the *design* of the optical field. Indeed, several interesting works[4–6] have shown the possibilities of controlling the selectivity of chemical reactions (and/or excitation) via manipulating the laser fields. However, in general, this requires the solution of an inverse problem, that is, for a given molecular system one designs a necessary pumping field for achieving the desired type of selective excitation (or reaction). To our knowledge there is no general methodology of this kind for optical field design. In a recent work[7] the treatment of magnetic resonance selective excitation has led to such an algorithm for rf-pulse design. A similar formalism for designing an optimal field for selective vibrational excitation is developed in the present work.

Selective vibrational excitation in a polyatomic system means achieving a desired bond-energy distribution with a minimum disturbance to the remainder of the system. Mathematically, this can be expressed in various ways. Since the dynamics of moleclar systems is governed by Schrödinger's equation, here we formulate the goal of selective vibrational excitation as a constrained optimization problem. This leads to the use of optimal control theory[8] which is devoted to dynamical optimization problems with differential equations as constraints. To illustrate how an optical field for selective vibrational excitation can be designed by virtue of optimal control theory, we restrict ouselves to the case of linear, harmonic chain molecules in this work. More general cases will be treated in a following paper.[9]

In Sec. II the problem of designing the optical field for selective vibrational excitation is formulated within the framework of the optimal control theory. Section III contains the detailed description of the procedure for computing the optimal field. As illustrative examples, a number of cases with various dipole distributions as well as selective excitation objectives are studied in Sec. IV. The sensitivity of the objectives with regard to errors in the optimal fields is analyzed in Sec. V. A discusision and brief remarks are included in Sec. VI.

II. FORMULATION

For the purpose of illustration let us consider a linear harmonic chain molecule consisting of $(N+1)$ atoms. The Hamiltonian for the molecule is given by

$$H_0 = T + V = \tfrac{1}{2}\mathbf{p}^T\mathbf{G}\mathbf{p} + \tfrac{1}{2}\mathbf{q}^T\mathbf{F}\mathbf{q}, \tag{2.1}$$

where the superscript T denotes the transpose, the vectors $\mathbf{q}$ and $\mathbf{p}$ are bond displacements and the corresponding momenta, respectively; $\mathbf{F}$ is a diagonal force constant matrix with elements $F_{ij} = \delta_{i,j}k_i$ and k_i is the force constant for the bond i; the $\mathbf{G}$ matrix has the elements

$$G_{ij} = \delta_{i,j}(\mu_{i+1} + \mu_i) - \delta_{i,(j+1)}\mu_i - \delta_{i,(j-1)}\mu_{i+1} = G_{ji},$$

where $\mu_i = 1/m_i$ with m_i being the mass of ith atom. If the external optical field is described classically, the total Hamiltonian for the molecule in the external field $\epsilon(t)$ with the polarization along the molecular chain reads

$$H = H_0 + H_{\text{in}} = \tfrac{1}{2}\mathbf{p}^T\mathbf{G}\mathbf{p} + \tfrac{1}{2}\mathbf{q}^T\mathbf{F}\mathbf{q} - \epsilon(t)D(\mathbf{q}), \tag{2.2}$$

where $D(\mathbf{q})$ is the molecular dipole function. If the dipole of the molecule is approximated as

$$D(\mathbf{q}) = D(\mathbf{O}) + \left[\frac{\partial D}{\partial \mathbf{q}}\Big|_{\mathbf{q}=\mathbf{o}}\right]\mathbf{q} \tag{2.3}$$

with $\partial D/\partial \mathbf{q} = (\partial D/\partial q_1, \ldots, \partial D/\partial q_N)$ being a row vector, the equations of motion for the quantum expectation values of $\langle \mathbf{q}(t) \rangle$ and $\langle \mathbf{p}(t) \rangle$ have the form

 0021-9606/88/116870-14$02.10

$$\langle \dot{\mathbf{q}}(t)\rangle = \mathbf{G}\langle \mathbf{p}(t)\rangle, \tag{2.4a}$$

$$\langle \dot{\mathbf{p}}(t)\rangle = -\mathbf{F}\langle \mathbf{q}(t)\rangle + \epsilon(t)\left(\frac{\partial D}{\partial \mathbf{q}}\Big|_{\mathbf{q}=\mathbf{o}}\right)^T. \tag{2.4b}$$

Introducing a new column $2N$-vector $\mathbf{z}(t)$,

$$\mathbf{z}(t) = \begin{pmatrix} \langle \mathbf{q}(t)\rangle \\ \langle \mathbf{p}(t)\rangle \end{pmatrix}, \tag{2.5}$$

one can rewrite Eqs. (2.4) as

$$\dot{\mathbf{z}}(t) = \mathbf{A}\mathbf{z} + \epsilon(t)\mathbf{b} \tag{2.6a}$$

with

$$\mathbf{A} = \begin{pmatrix} \mathbf{O} & \mathbf{G} \\ -\mathbf{F} & \mathbf{O} \end{pmatrix} \tag{2.6b}$$

and

$$\mathbf{b} = \begin{pmatrix} \mathbf{o} \\ \left(\dfrac{\partial D}{\partial \mathbf{q}}\Big|_{\mathbf{q}=\mathbf{o}}\right)^T \end{pmatrix}, \tag{2.6c}$$

where $\mathbf{o}$ and $\mathbf{O}$ are an N-dimensional zero vector and an $N\times N$ zero matrix, respectively. We assume that the molecule is in its ground state initially. Then the initial condition for $\mathbf{z}(t)$ reads

$$\mathbf{z}(0) = \mathbf{o}. \tag{2.7}$$

Without any approximation we may set the ground state energy of the molecule equal to zero, and one can then show that the energy for the molecule is given by

$$E_t = \tfrac{1}{2}\mathbf{z}^T(t)\mathbf{M}\mathbf{z}(t) \tag{2.8}$$

with

$$\mathbf{M} = \begin{pmatrix} \mathbf{F} & \mathbf{O} \\ \mathbf{O} & \mathbf{G} \end{pmatrix}. \tag{2.9}$$

We *define* the bond energy as

$$e_i(t) \equiv \tfrac{1}{2}k_i(\langle \mathbf{q}_i(t)\rangle)^2 + \tfrac{1}{2}G_{i2}(\langle \mathbf{p}_i(t)\rangle)^2. \tag{2.10}$$

The total energy of the molecule can be approximated as the sum of all the bond energy:

$$E_m(t) \simeq E_b = \sum_{i=1}^{N} e_i = \frac{1}{2}\mathbf{z}^T(t)\mathbf{M}_d\mathbf{z}(t) \tag{2.11}$$

with

$$\mathbf{M}_d = \begin{pmatrix} \mathbf{F} & \mathbf{O} \\ \mathbf{O} & \mathbf{G}_d \end{pmatrix} \tag{2.12}$$

where $\mathbf{G}_d$ denotes the diagonal part of the matrix $\mathbf{G}$.

We interprete selective excitation as requiring that at time T the expectation value $\langle q_s(T)\rangle$ of a particular bond s reach a specified value Q_s and the corresponding expectation value $\langle p_s(T)\rangle$ be positive. In addition, we require that the disturbance to the molecular system, i.e., the total energy of the molecular system should remain as small as possible during the time interval $0\leqslant t\leqslant T$. Moreover, since an important subsidiary aspect of selective excitation is to achieve the goal with a minimum of energy consumption from the pumping field, we thus also desire to minimize the energy fluence of the pumping field

$$E_\epsilon = \frac{1}{2}\int_0^T dt\,\epsilon^2(t).$$

Mathematically, the expectation values of $\mathbf{z}(t)$, the pump field energy E_ϵ, and the molecular energy $E_m(t)$ are functionals of the external field $\epsilon(t)$. Therefore, the above interpretation for selective vibrational excitation can be expressed as finding an optimal field which minimizes the objective functional J defined as

$$J = \Phi(T) + L$$

with

$$\Phi(T) = \frac{k_s}{2}(\langle q_s(T)\rangle - Q_s)^2 + \frac{1}{2}G_{ss}(\langle p_s(T)\rangle)^2 h(-\langle p_s(T)\rangle),$$

$$L = \int_0^T dt\left[\mathbf{w}^T\mathbf{e} + \tfrac{1}{2}w_e\epsilon^2(t)\right], \tag{2.13}$$

where the bond energy N-vector $\mathbf{e}$ has elements e_i with weight vector $\mathbf{w}$, the weight factor for E_ϵ is w_e, and $h(x)$ is the step function

$$h(x) = \begin{cases} 1 & \text{if } x>0 \\ 0 & \text{if } x<0 \end{cases}.$$

It is obvious that the error function $\Phi(T)$ measures the degree of satisfaction of the objectives while the cost function L adds in the total disturbance to the molecular system and the energy expended. The choice of weight factors $\mathbf{w}$ and w_e allows for flexibility in balancing the contributions to J. It should be noted that this is a constrained minimization problem, because the expectation values $\mathbf{z}(t)$ have to satisfy the equations of motion, Eqs. (2.6). It is well known that a constrained minimization problem can be treated as an unconstrained one by introducing Lagrange multipliers, that is, instead of minimizing J with constraint Eqs. (2.6) one minimizes the modified objective functional

$$\bar{J} = J - \int_0^T dt\,\boldsymbol{\lambda}^T(t)[\dot{\mathbf{z}}(t) - \mathbf{A}\mathbf{z}(t) - \epsilon(t)\mathbf{b}] \tag{2.14}$$

with no constraint. The Lagrange $2N$-vector $\boldsymbol{\lambda}(t)$ is at this point arbitrary. It is clear, however, that for any choice of $\boldsymbol{\lambda}(t)$ the value of $\bar{J}$ is the same as that of J for any $\mathbf{z}(t)$ and $\epsilon(t)$ satisfying Eqs. (2.6). The flexibility in the choice of $\boldsymbol{\lambda}(t)$ can then be used to make the problem as simple as possible.

Suppose that an arbitrary variation $\delta\epsilon(t)$ leads to a variation $\delta\mathbf{z}(t)$, then the corresponding variation $\delta\bar{J}$ is given by

$$\delta\bar{J} = I + II, \quad I = \frac{\partial\Phi(T)}{\partial\mathbf{z}(T)}\delta\mathbf{z}(T),$$

$$II = \int_0^T dt\left\{\left[\mathbf{w}^T\frac{\partial\mathbf{e}(t)}{\partial\mathbf{z}(t)} + \boldsymbol{\lambda}^T(t)\mathbf{A}\right]\delta\mathbf{z}(t) - \boldsymbol{\lambda}^T(t)\delta\dot{\mathbf{z}}(t) + [w_e\epsilon(t) + \boldsymbol{\lambda}^T(t)\mathbf{b}]\delta\epsilon(t)\right\}. \tag{2.15}$$

Now if we notice that $\delta\mathbf{z}(0) = \mathbf{o}$ and select $\boldsymbol{\lambda}(t)$ as the solution to the adjoint differential equation

$$\dot{\boldsymbol{\lambda}}(t) = -\mathbf{A}^T\boldsymbol{\lambda}(t) - \mathbf{W}_b\mathbf{M}_d\mathbf{z}(t), \tag{2.16a}$$

where the diagonal weight matrix has elements

$$[\mathbf{W}_b]_{ij} = [\mathbf{W}_b]_{(i+N)(j+N)} = \delta_{i,j}w_i,$$
$$\text{with } i = 1,\ldots,N \tag{2.16b}$$

and the final condition on Eqs. (2.16) is

$$\lambda(T) = \left(\frac{\partial \Phi(T)}{\partial \mathbf{z}(T)}\right)^T \tag{2.17a}$$

with

$$\left(\frac{\partial \Phi(T)}{\partial \mathbf{z}(T)}\right)_i = \delta_{i,s}[k_s(\langle q_s\rangle(T) - Q_s)] + \delta_{i,(s+N)} G_{ii}\langle p_s(T)\rangle h(-\langle p_s(T)\rangle), \tag{2.17b}$$

then we have

$$\delta\bar{J} = \int_0^T dt\,[w_e\epsilon(t) + \lambda^T(t)\mathbf{b}]\delta\epsilon(t) \tag{2.18a}$$

or

$$\frac{\delta\bar{J}}{\delta\epsilon(t)} = w_e\epsilon(t) + \lambda^T(t)\mathbf{b}. \tag{2.18b}$$

The problem of finding a field which will minimize the $\bar{J}$ thus becomes one of searching for a field which will satisfy

$$\frac{\delta\bar{J}}{\delta\epsilon(t)} = w_e\epsilon(t) + \lambda^T(t)\mathbf{b} = 0, \tag{2.19}$$

where $\lambda(t)$ satisfies Eqs. (2.16) with the final condition Eqs. (2.17), while $\mathbf{z}(t)$ satisfies Eqs. (2.6) with the initial condition Eq. (2.7). In other words, we have to solve Eqs. (2.6) and (2.16) which are coupled by the minimum condition Eq. (2.19). Note that this is a two-point boundary value problem: the initial condition for $\mathbf{z}(t)$ at $t = 0$ is given while the final condition for $\lambda(t)$ at $t = T$ is specified. To solve this kind of the problem is a difficult task computationally. One has to resort to minimization algorithms. In this work the conjugate gradient algorithm[10] is used. The detailed computational procedure will be presented in the following section.

III. COMPUTATIONAL PROCEDURE

Since we can not directly integrate Eqs. (2.6) and (2.16) coupled through Eq. (2.19) due to the unknown $\epsilon(t)$, an iterative scheme based on the conjugate gradiant algorithm is adapted to find $\epsilon(t)$. First, we discretize $\epsilon(t)$ into a set of N_T variables $\epsilon_i = \epsilon(t_i)$, $i = 0,...,N_T$ with $t_i = i(T/N_T)$ for a sufficiently large number N_T. Thus the functional derivative (2.19) becomes a set of multivariable partial derivatives

$$\frac{\partial\bar{J}}{\partial\epsilon_i} = [w_e\epsilon_i + \lambda^T(t_i)\mathbf{b}]\Delta t, \quad i = 0,...,N_T, \tag{3.1}$$

or in vector form

$$\mathbf{g} \equiv \left(\frac{\partial\bar{J}}{\partial\boldsymbol{\epsilon}}\right)^T = (w_e\boldsymbol{\epsilon} + \Lambda\mathbf{b})\Delta t \tag{3.2}$$

with

$$(\mathbf{g})_i = \frac{\partial\bar{J}}{\partial\epsilon_i}, \quad (\boldsymbol{\epsilon})_i = \epsilon_i, \tag{3.3a}$$

$$(\Lambda)_{ij} = \lambda_j(t_i), \quad \Delta t = T/N_T. \tag{3.3b}$$

Starting with an intelligently guessed $\epsilon^{(o)}$ we can integrate Eqs. (2.6) with the initial condition (2.7) from $t = 0$ to $t = T$, since there is no explicit dependence on $\lambda(t)$ in Eq. (2.6). Then, the final condition for $\lambda(t)$ at $t = T$ is calculated according to Eq. (2.17) and Eq. (2.16a) is integrated backwards from $t = T$ to $t = 0$ to obtain Λ. Finally, Λ and $\mathbf{z}(t)$ are used to calculate the gradient vector $\mathbf{g}$ and the objective functional J according Eqs. (3.2) and (2.13). By using the conjugate gradient algorithm one can determine a new field vector $\epsilon^{(1)}$ for the next iteration. This iteration procedure is repeated until the error criteria $\mathbf{g}^T\mathbf{g} < \sigma$ is satisfied for a specified tolerance σ. It is interesting to note that the Lagrange multipliers $\lambda(t)$ represent the feedback from the desired objective and certainly should flow backwards in time. Due to this feedback, the iterative procedure converges rather rapidly and is insensitive to the initial guess of the field $\epsilon(t)^{(o)}$ in the cases studied here. In other contexts, $\lambda(t)$ has been referred to as the importance function.[11]

It should be noted that for the system discussed in the present work the optimal field can directly be found via solving the corresponding Riccati equation[8] if we require $\langle p_s(T)\rangle = P_s$ instead of the requirement $\langle p_s(T)\rangle > 0$.

IV. ILLUSTRATIVE EXAMPLES

In this section we consider three examples to illustrate how the algorithm developed above can be used to *design* an optical field for achieving selective vibrational excitation in polyatomic molecules. In all these examples, we set all the cost weight factors equal to 1 except for the target bond weight which is set to zero, since we do not have any preference among the contributions to the cost funciton L and the target bond is treated separately in $\Phi(T)$.

(i) Ten atom linear harmonic chain: The model system consists of ten atoms each with equal mass $m = 10$ amu. The force constants for the nine bonds are equal and have the value $k = 1.15$ a.u. We assume that only one end bond, the ninth bond, has a dipole D with $\partial D/\partial q_9 = 0.295$ a.u. The objective is to excite the first bond at the other end. To achieve this objective, a value for Q_1 is specified. There are two reasons why we choose this system. First, for this system we have analytic expressions for the normal mode frequencies

$$\omega_n = 2\sqrt{\frac{k}{m}}\sin\frac{n\pi}{2(N+1)}, \quad n = 1,...,N, \tag{4.1a}$$

and corresponding eigenvectors

$$Y_k^n = C_n \sin k\frac{n\pi}{N+1}, \quad k = 1,...,N \text{ and } n = 1,...,N, \tag{4.1b}$$

with $N = 9$ in this case, where C_n is a normalization constant. Second, the two end bonds have the same local mode frequencies which also happen to be exactly equal to the fifth normal mode frequency in this case. Therefore, this system provides a very challenging test case for selective local bond excitation. To appreciate this point, we plot in Fig. 1 the local bond energy as a function of time and bond number, when a single mode laser with a frequency equal to the local end bond frequency 2456 cm^{-1} is used to pump the system. It is clearly seen that after a transient period ~ 0.05 ps, the single mode pumping results in the excitation of the fifth normal mode in which the energy is equally distributed among the odd number bonds while the even number bonds remain unexcited. There certainly is no sign of local excitation.

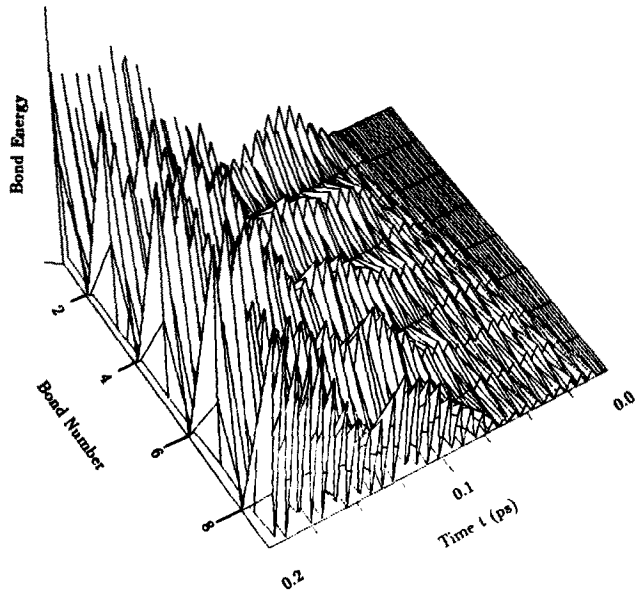

FIG. 1. Bond energy as a function of time and bond number for the system of example (i) pumped by a single mode nonoptimally designed laser with the local mode frequency 2546 cm^{-1}. This frequency is also equal to the fifth normal mode frequency. The energy is equally distributed among the odd number bonds while the even number bonds are nodes. Comparison should be made with the optimal result of Fig. 2.

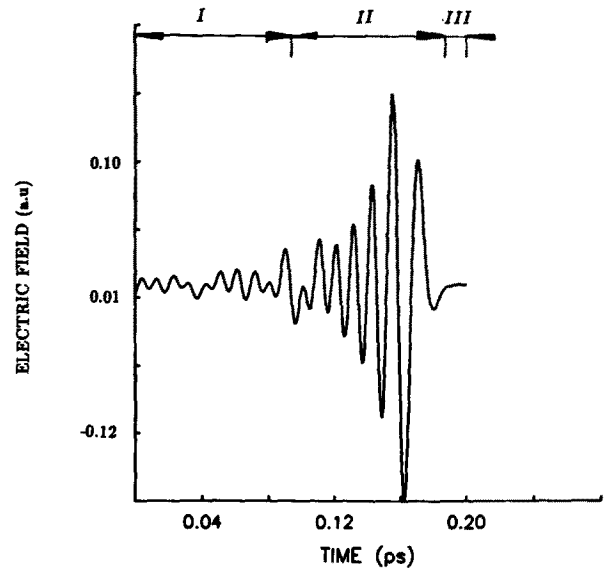

FIG. 3. The designed optimal field for the time interval $T = 0.2$ ps. The field consists of three stages: the low intensity first period, the high intensity second pumping period, and the turned off third period.

We now see results from the optimal control approach. Figure 2 shows the optimally controlled bond energy as a function of time and bond number. It is seen that at time $t = T = 0.2$ ps, almost all the energy is localized at the first bond which is our objective, while for $t < T$ there is much less energy in each of the other bonds. In other words, selective local excitation is well achieved. The corresponding optimal field is presented in Fig. 3. Note that the optimal field has structure on the time scale of ~ 10 fs which is approximately equal to the vibrational period. The field basically consists of three stages. During the first period out to ~ 0.09 ps, the field intensity is very low and little energy is deposited in the molecule, but the relative phase of the expectation values $\langle \mathbf{q}(t) \rangle$ and $\langle \mathbf{p}(t) \rangle$ are being adjusted in preparation for the intense pumping to follow in the second period. The main pumping occurs in the second period ($\sim 0.09 \leqslant t \leqslant \sim 0.19$ ps). The molecule signals the field to be turned off during the third period ($\sim 0.19 \leqslant t \leqslant 0.2$ ps). It should be realized that we have not explicitly demanded that the field be turned off near the end of the time interval T. The physical content of the optimal algorithm automatically gives rise to this feature. Any energy deposited into the ninth bond near the end of the time interval T will never reach the first bond and should not be deposited in order to minimize the energy fluence of the field as we demanded. Thus, this feature in the resultant optimal field is good evidence of the effectiveness of the optimization algorithm. An examination of Fig. 2 clearly reveals that the pump field generates a "molecular acoustic pulse" that travels from one end of the molecule to the other.

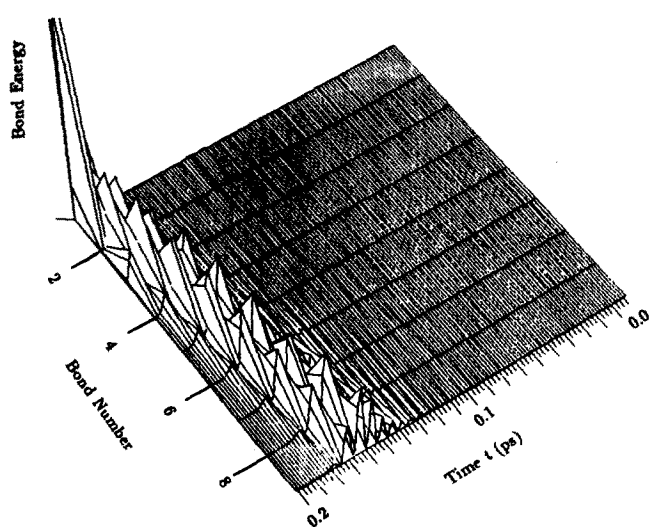

FIG. 2. Bond energy as a function of time and bond number for the system of illustration example (i) pumped by a *designed* optimal field. The local excitation at the first bond is now successfully achieved.

For the purpose of local excitation, generally there is no physical reason for specifying a particular value of the time interval T. To see how the value of the time interval T affects the resultant optimal field, four optimal fields as functions of time t for different T are plotted in Fig. 4. Except for the very short time interval $T = 0.05$ ps, roughly all the fields consist of three stages and have almost the same second and third stages. That is, the only difference is the length of the first period during which the intensity of the field is low. The field intensity in the second period decreases with an increase of the value of T, but the decrement diminishes rapidly. To see this more clearly, the two optimal fields for the time interval $T = 0.4$ ps and $T = 0.2$ ps, respectively, are superimposed on each other in Fig. 5 over the last 0.2 ps. Therefore, for $T > 0.2$ ps increasing T basically only leads to lengthening the first period when the amplitude approaches zero. In this sense, for sufficiently large T (> 0.2 ps in this case) the resultant field $\epsilon(t) = \epsilon'(T - t)$ as a function of $(T - t)$ has con-

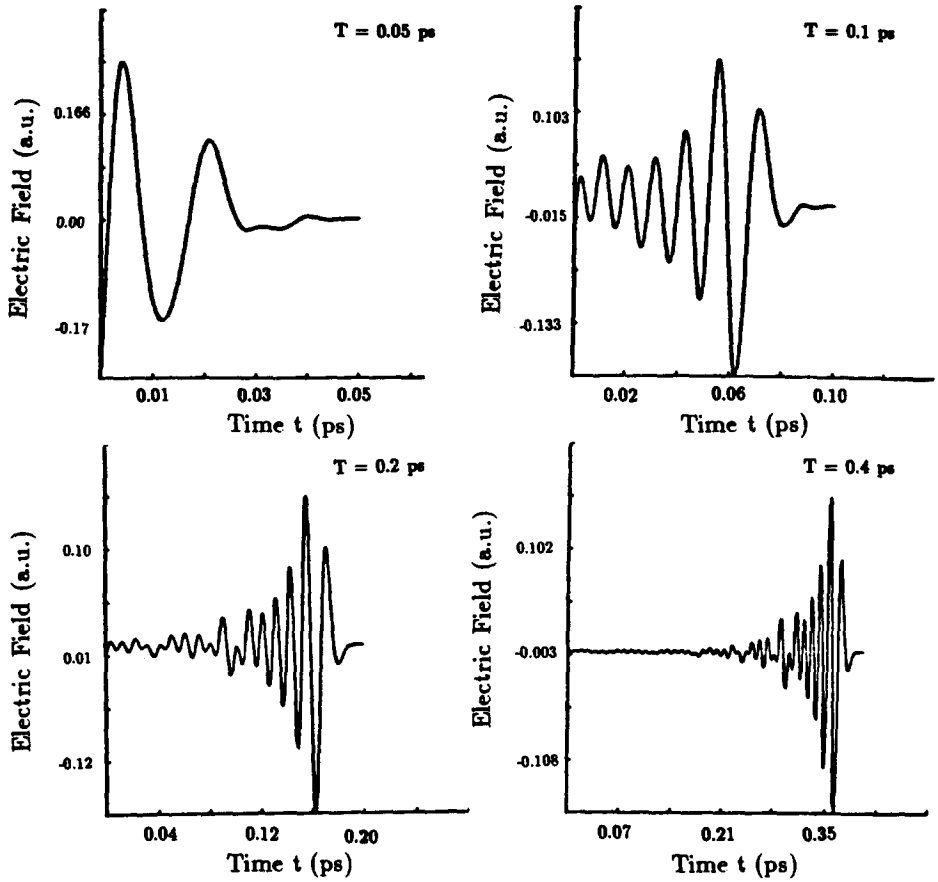

FIG. 4. The optimal fields for four different time intervals. It is evident that except for the one with $T = 0.05$ ps all the fields have essentially the same second and third periods.

verged and is *unique for a given objective functional.* The optimal field pulse is short (~ 0.1 ps) and intense ($\sim 10^{14}$ W/cm^2 at the peak intensity) under the present constraint of minimum energy fluence of the field.

The power spectrum as well as the sine and cosine Fourier transforms of the optimal field for $T = 0.5$ ps along with the normal mode frequencies are shown in Fig. 6. For $T = 0.5$ ps the resolution of the spectrum $\Delta\omega$ is about 67 cm^{-1}, and one can see that the power spectrum is a broad band with some resolved peaks which coincide with the normal mode frequency lines within the resolution of the spectrum. The most intense peak corresponds to the fifth normal mode. The visible peak frequencies of the power spectrum and the normal mode frequencies are listed in Table I for comparison. The broad band spectrum is due to the power broadening of the very intense field. To see how the normal modes are pumped by the optimal field the normal mode energy as a function of time and mode number is plotted in Fig. 7. It is seen that the high frequency modes are excited first. Then the excitation gradually spreads to the low frequency modes. At the end of the time interval $T = 0.2$ ps the fifth mode has the highest excitation.

In this example case we find that the optimal pumping field is complicated both in the time and frequency domains. To achieve the objectives one has to treat the complete molecule–radiation system dynamics and coherently excite the molecular modes in a cooperative way. This theme was found in all the cases studied including others not reported in this paper.

(ii) Middle bond stretch of 20 atom linear harmonic chain: The system consists of 20 atoms each with equal mass

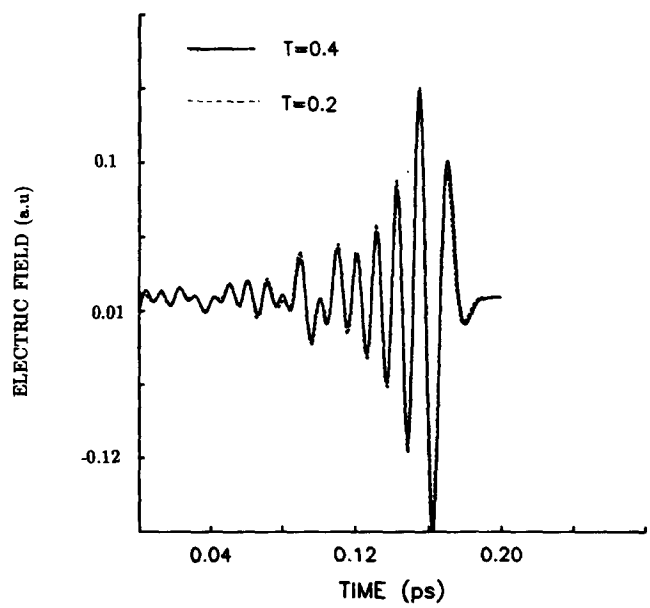

FIG. 5. Comparison of the optimal fields for the time intervals $T = 0.2$ ps and $T = 0.4$ ps. The field as a function of $(T - t)$ becomes independent of T.

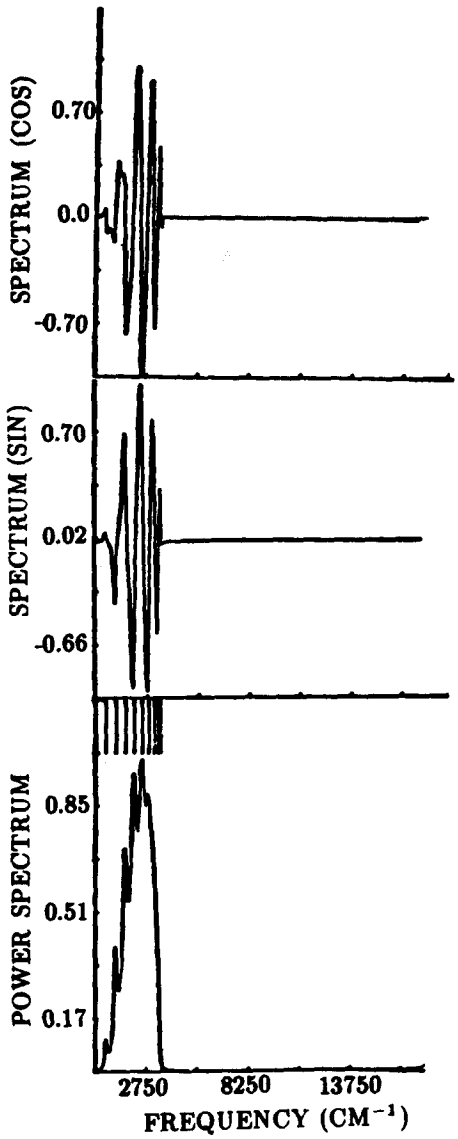

FIG. 6. The cosine and sine Fourier transforms as well as the power spectrum of the optimal field for the time interval $T = 0.5$ ps. The spectrum has a broad band structure with resolved peaks coinciding with the normal mode frequencies.

$m = 10$ amu. Again, the force constants for all bonds are same and equal to $k = 1.15$ a.u. Only one end, the nineteenth bond has a dipole with $\partial D_{19}/\partial q_{19} = 0.295$ a.u. The objective is to locally excite the middle tenth bond, therefore corresponding to the concerted movement of the left and right halves of the molecule in opposite directions at time T. In this case the end bond local mode frequency (~ 2465 cm^{-1}) corresponds to tenth normal mode frequency. However for the tenth normal mode the tenth bond is a node. Therefore, if a single mode laser with the frequency 2465 cm^{-1} is used to pump the molecule, the tenth normal mode will be excited as shown in Fig. 8. One sees in this case that not only does the

TABLE I. Comparison of normal mode frequencies and spectral peak of the optimal field of illustration (i).

Normal mode	Spectral peak[a]
535	533
1077	1067
1582	1601
2049	2068
2465	2478
2820	2801
3106	
3315	
3443	

[a] The resolution $\Delta\omega = 66$ cm^{-1}.

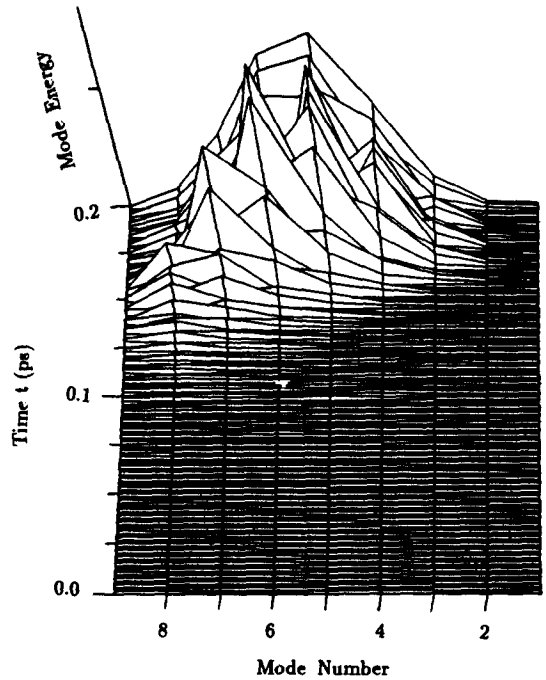

FIG. 7. The normal mode energy as a function of time and mode number for the system of example (i) pumped by the optimal field. The coherent excitation of the normal modes is evident.

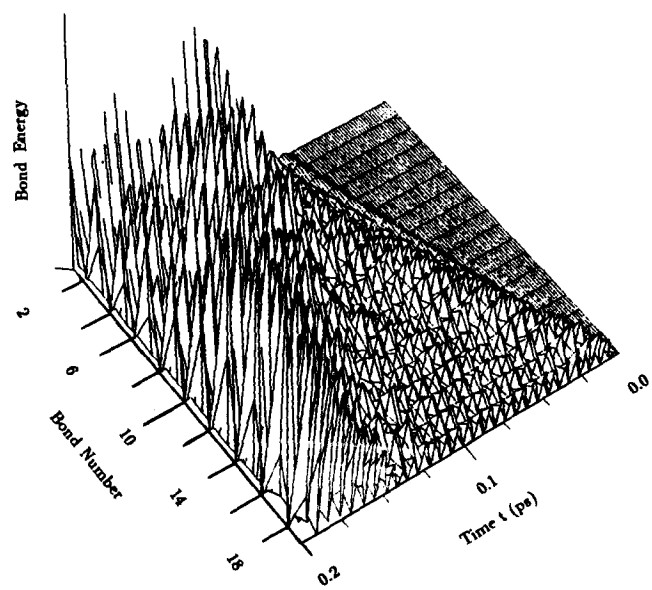

FIG. 8. Bond energy as a function of time and bond number for the system of illustration (ii) pumped by a single mode nonoptimally designed laser with the local mode frequency 2546 cm^{-1}. This frequency is also equal to the tenth normal mode frequency. The energy is equally distributed among the odd number bonds while all the even number bonds are unexcited. Comparison should be made with the optimal result of Fig. 10.

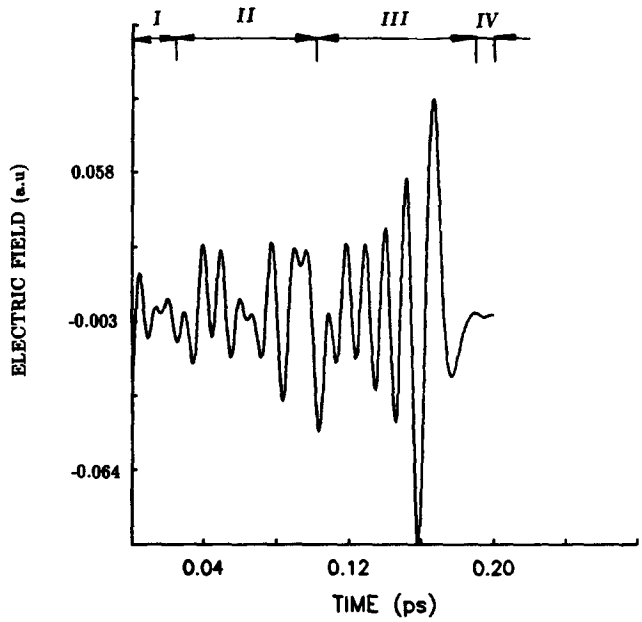

FIG. 9. The *designed* optimal field for the example system (ii). There are four stages with a null fourth period.

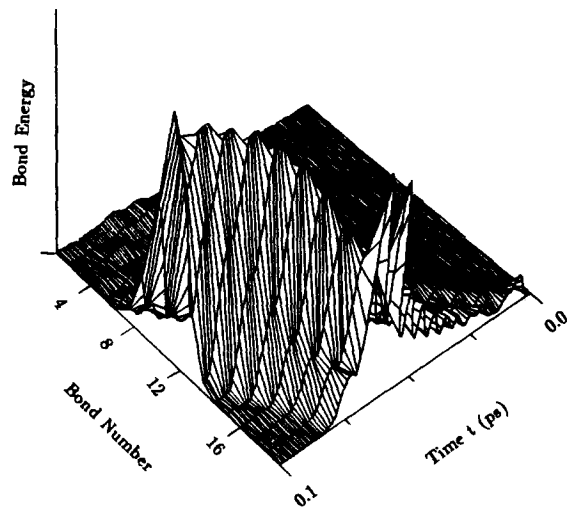

FIG. 11. The bond energy as a function of time and bond number for the example system (ii) pumped by the designed optimal field with the time interval $T = 0.1$ ps. The disturbance to the other bonds is comparable to the target bond and thus unacceptable for this short T case.

energy spread over all the odd number bonds, but also the objective bond, the tenth bond, receives no energy at all. It is obvious that one has to pump all the normal modes coherently in a particular way so that at time T an adequate superposition of all excited modes will give rise to the desired local excitation. There is certainly no chance that one will be able to guess at the pumping scheme for achieving this goal. Figures 9 and 10 show the optimal field obtained by the approach in Sec. III and the corresponding local bond energies as functions of time t. The pumping field consists of four stages and very cleverly generates a strong local excitation at the target bond. As in the last example, the phase of the molecular motion is adjusted in the first low intensity period. It is this period that will be lengthened when the time interval T is increased. During the second period of pumping, when the field intensity is also rather low, a local excitation "acoustic wave" is generated such that it propagates from the pump end bond to the other end bond, ultimately being reflected back and reaching the target bond at time T. The high intensity field does most of the pumping in the third period and generates a second acoustic wave of local excitation, which is much stronger than the first one. This second acoustic wave meets the first reflected "wave" at the target bond at time T and generates a strong local excitation there as shown in Fig. 10. The molecule signals the field to be turned off in the fourth period, as it did in example (i), to minimize the energy fluence of the pumping field; once again no energy deposited at the nineteenth bond can reach the target bond in this period. The "head-on collision" of two waves at the target bond is a very efficient way to generate a strong local excitation. To see the effectiveness of this head-on collision more clearly, in Fig. 11 the bond energy as a function of time and bond number is plotted for $T = 0.1$ ps. Comparing Fig. 11 with Fig. 10 one finds that for the case $T = 0.1$ ps the pumping pulse is too short to generate a significant reflected wave so that the resultant local excitation at the target bond is much less pronounced (i.e., an undesirable broad distribution of bonds are excited for the shorter pulse) than it is for the case $T = 0.2$ ps. Therefore, for pumping to be efficient, the time interval T must be longer than 0.2 ps.

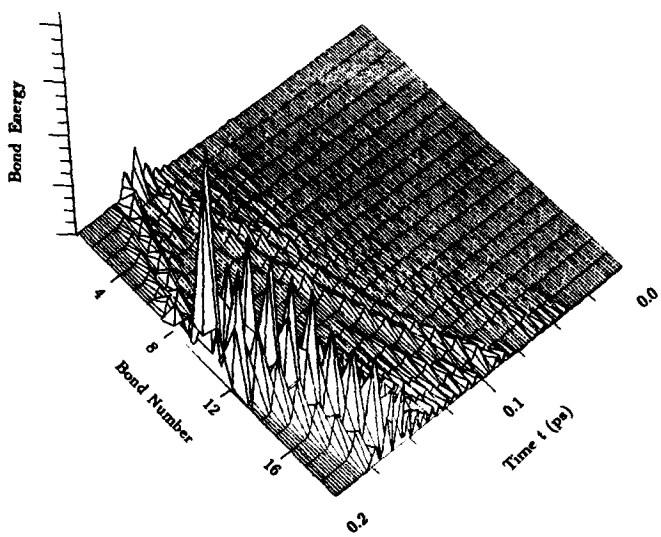

FIG. 10. The bond energy as a function of time and bond number for the example system (ii) pumped by the *designed* optimal field with the time interval $T = 0.2$ps. The local excitation at the tenth bond is successfully achieved in an unusual fashion. The disturbance to the remainder of the molecule is small.

The power spectrum as well as the sine and cosine Fourier transforms of the optimal field for $T = 0.2$ ps along with the normal mode frequencies are given in Fig. 12. It is seen that the power spectrum has a broad band structure with apparent peaks corresponding to only a portion of the odd number normal mode frequencies. In Table II the normal mode frequencies and the peak frequencies of the power spectrum of the optimal field are listed for comparison. Once

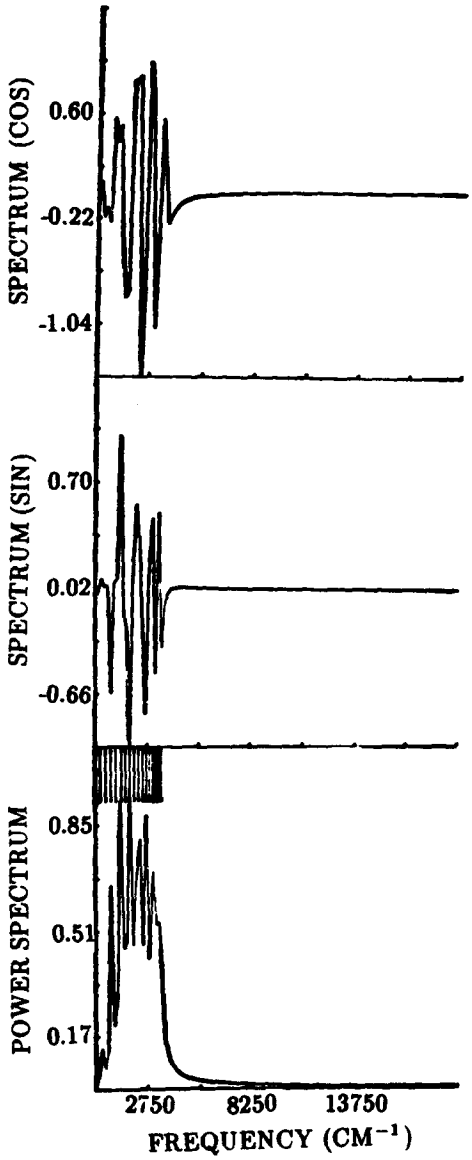

FIG. 12. The cosine and sine Fourier transforms and the power spectrum of the designed optimal field for the time interval $T = 0.2$ ps in example system (ii). The spectrum has a broad band structure with the peaks corresponding only to the odd number normal modes.

more one sees that the algorithm generates a surprisingly "clever" pumping field: the optimal field includes almost no frequency components corresponding to the even number normal modes which have no contribution to the target bond stretch. Consequently, as shown in Fig. 13 essentially only the odd number normal modes are pumped.

(iii) Ten atom linear harmonic chain with two end dipoles: The purpose of this case study is to see how well the optimal field designed by the present algorithm selectively excites one of two similar bonds in the same molecule. We first consider a linear chain molecule consisting of ten atoms with each atom having the same mass $m = 10$ amu except for the atom 1 which has a variable mass m_1. All bonds have the same force constant $k = 1.15$ a.u. Only the two end bonds have dipoles which have the same functional form with $\partial D_1/\partial q_1 = \partial D_9/\partial q_9 = 0.295$ a.u. The objective is to locally excite the first bond while minimally disturbing the remainder of the molecule, especially bond number nine. The mass m_1 has been given six different values such that the reduced mass for the first bond stretch has the values $\mu_1 = 5$, 4.5, 4.0, 3.5, 3.0, and 2.5 amu, respectively. Note that the reduced mass $\mu_1 = 5$ amu corresponds to the mass $m_1 = 10$ amu. That is, in this case all the atom masses are equal. The optimal fields and the corresponding power spectra for these cases with $T = 0.2$ ps are given in Figs. 14 and 15, respective-

TABLE II. Comparison of normal mode frequencies and spectral peak of the optimal field of illustration (ii).

Normal mode	Spectral peak[a]
273	333
535	
813	833
1077	
1369	1334
1582	
1821	1834
2049	
2264	2334
2465	
2651	2668
2820	
2972	3002
3106	
3221	
3315	
3443	
3475	

[a]The resolution $\Delta\omega = 166$ cm^{-1}.

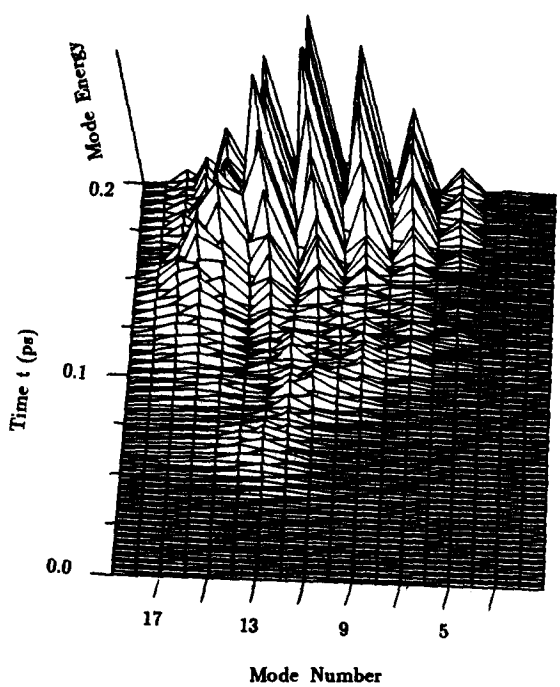

FIG. 13. The normal mode energy as a function of time and mode number for the system of illustration (ii) pumped by the optimal field. Essentially, only odd number normal modes are coherently excited.

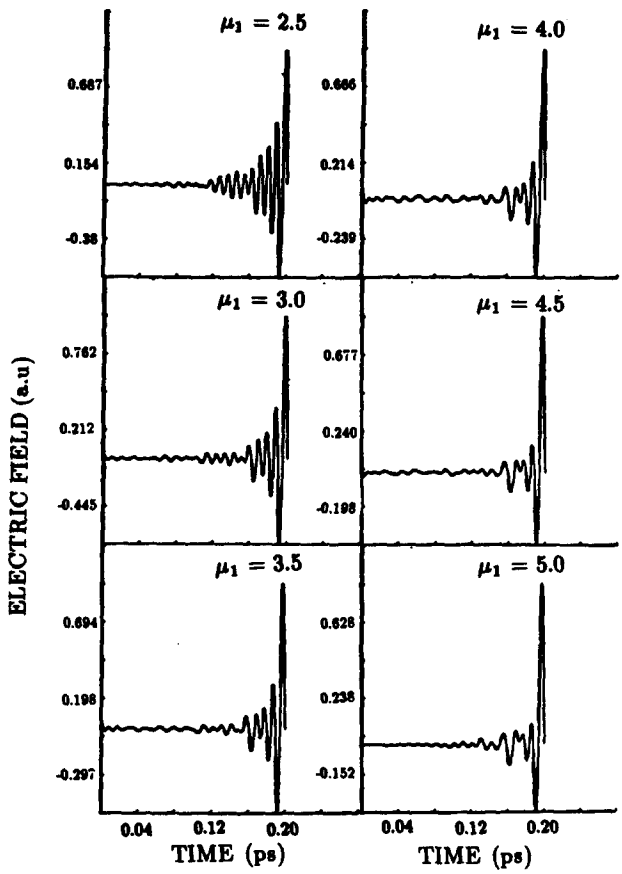

FIG. 14. The optimal fields for the different values of the reduced mass μ_1 of example system (iii). All the fields have only two stages with a high intensity second period following a low intensity phase adjustment period.

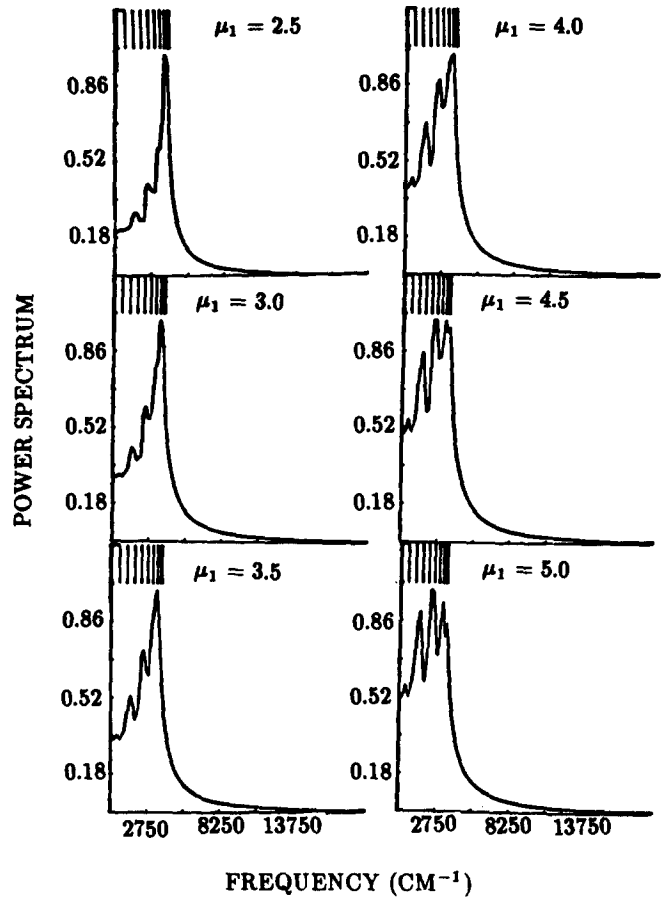

FIG. 15. The power spectra of the optimal fields for the different values of the reduced mass μ_1 of Sec. IV C. The apparent peaks correspond only to the odd number normal modes.

ly. It is seen that there is no period of null field near the end time T since the target bond can be directly pumped. The optimal fields only have two stages: one low intensity period of phase adjustment and one intense pumping period. Again, the spectra have broad band structure due to the high intensity of the short pumping pulse. It is interesting to see that there are only five peaks in the power spectrum which correspond to the odd number normal modes. This is physically understandable because for the even number normal modes the bond displacements and therefore the dipoles of the two end bonds have opposite signs. Consequently, energy can not be efficiently deposited into the molecule through the even number normal modes. It once more shows that execution of the present optimal control algorithm produced a "clever" field, since it *automatically* excludes the even number normal mode frequency components. It is also seen that the high frequency component of the optimal field, which corresponds to the ninth normal mode, becomes more dominant when the mass m_1 gets smaller. Physically, this is due to the fact that the local mode corresponding to the first bond stretch has a bigger component in the high frequency, ninth, normal mode when the mass m_1 becomes smaller. Figure 16 shows the bond energy distribution among the bonds for the different μ_1 values. The final stretchs of the target bond (first bond) and the ninth bond as functions of the reduced mass μ_1 are plotted in Fig. 17 for comparison. Note that for the reduced mass $\mu_1 = 5$ amu, there is no differentiation attained between the target bond and the ninth bond, since the two bonds are identical. On the other hand, for the reduced mass $\mu_1 = 2.5$ amu, the selective excitation of the target bond is achieved quite successfully.

To proceed one step further, we vary the first bond force constant k_1 along with mass m_1 so that the local mode frequencies for the target bond and the ninth bond are kept the same. This case serves the purpose of the testing whether the present optimal control approach can produce optimal fields which selectively excite only the target (first) bond even when the competing bond has the same local mode frequency. Figures 18 and 19 present the resultant optimal pumping fields, the power spectra of the fields, and the corresponding bond energies for two sets of combinations ($\mu_1 = 2.5$ amu, $k_1 = 0.575$ a.u.) and ($\mu_1 = 7.5$ amu, $k_1 = 1.725$ a.u.). One immediately finds that the two optimal fields and the power spectra are quite different and that the selective excitation of the target bond is successfully achieved for the combination in Fig. 18 ($\mu_1 = 2.5$ amu, $k_1 = 0.575$ a.u.), but less so for the combination in Fig. 19 ($\mu_1 = 7.5$ amu, $k_1 = 1.725$ a.u.). The results in Fig. 14–19 suggest that although the local mode frequencies have a role, the fundamental parameters such as mass and bond strength may be more important for deter-

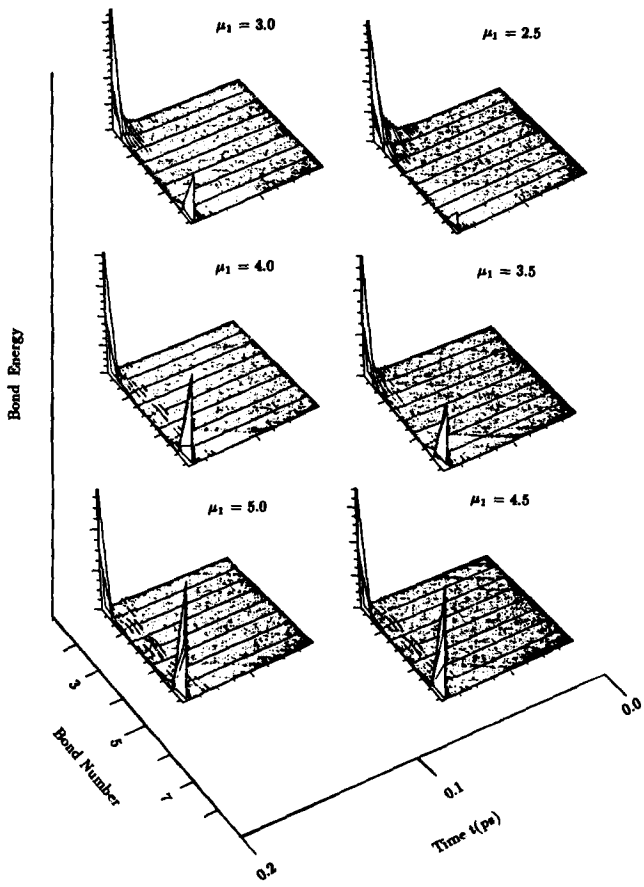

FIG. 16. The bond energy distribution among the bonds as functions of time for the different values of the reduced mass μ_1 of Sec. IV PC. For the case of $\mu_1 = 5$ amu there is no selective excitation attained while the local excitation at the first bond is achieved quite well for the case of $\mu_1 = 2.5$ amu.

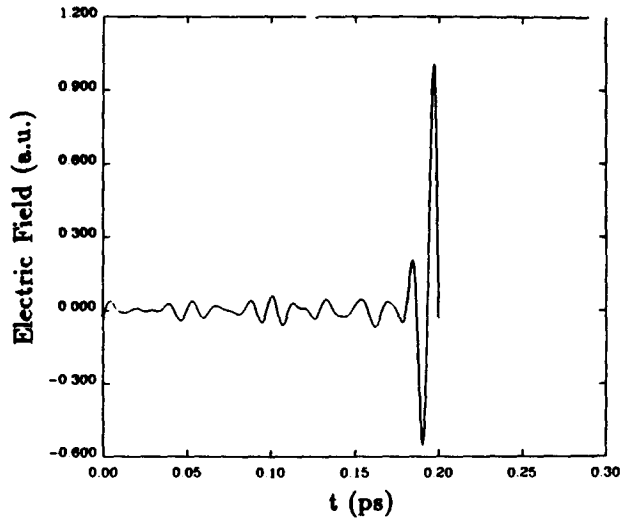

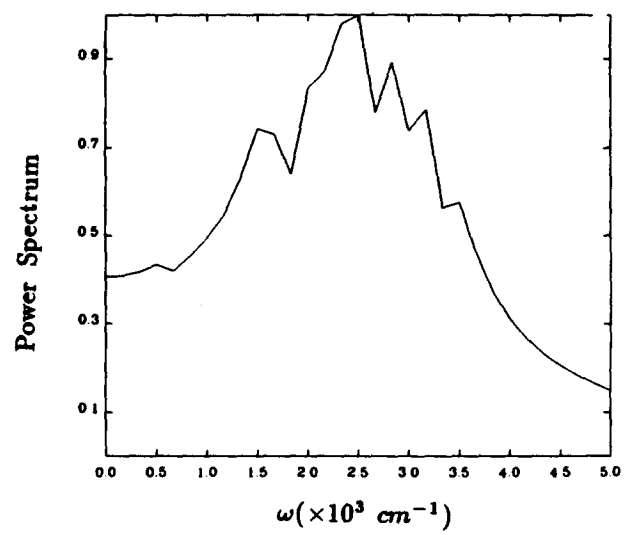

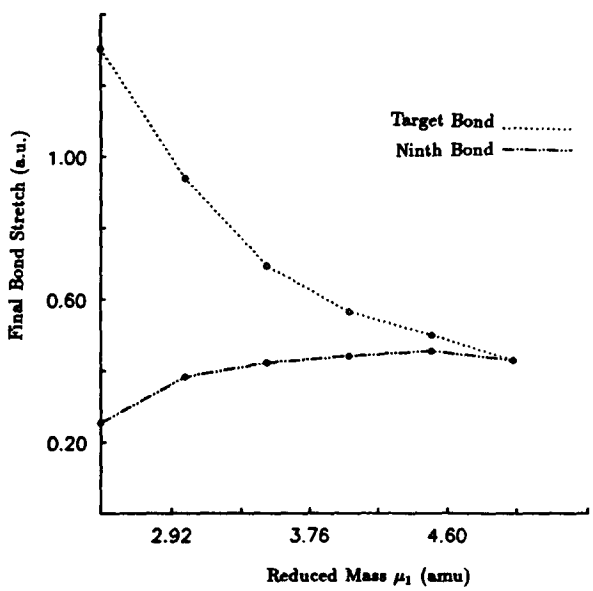

FIG. 17. The comparison of the final stretches of the target (first) bond and the ninth bond as functions of the reduced mass μ_1 for the example system (iii).

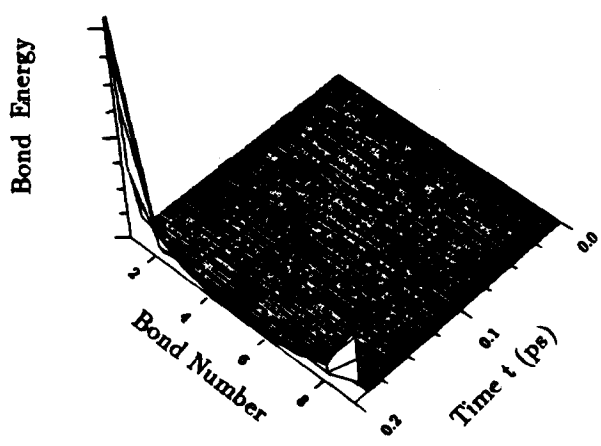

FIG. 18. The optimal field, power spectrum, and the bond energies for the combination ($\mu_1 = 2.5$ amu, $k_1 = 0.575$ a.u.). The local excitation is successfully achieved in spite of the fact that the two bonds have the same local mode frequencies.

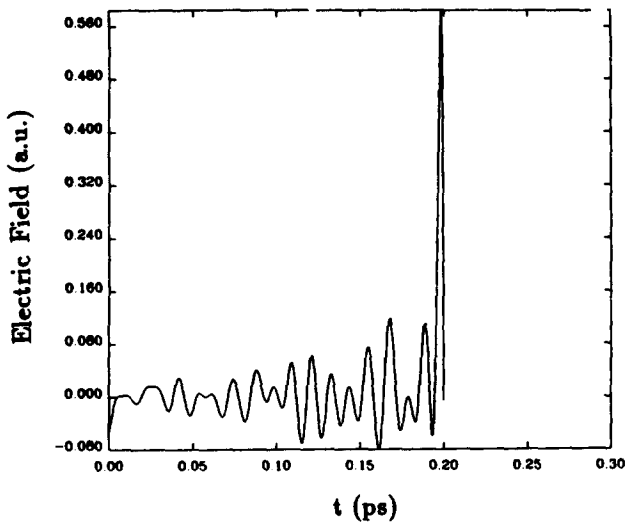

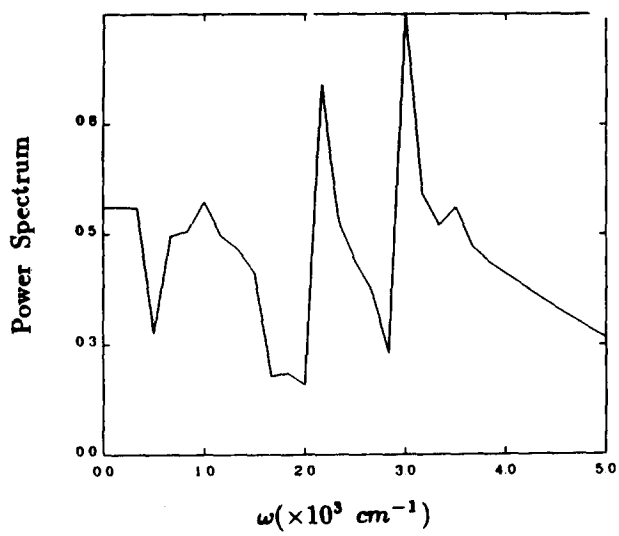

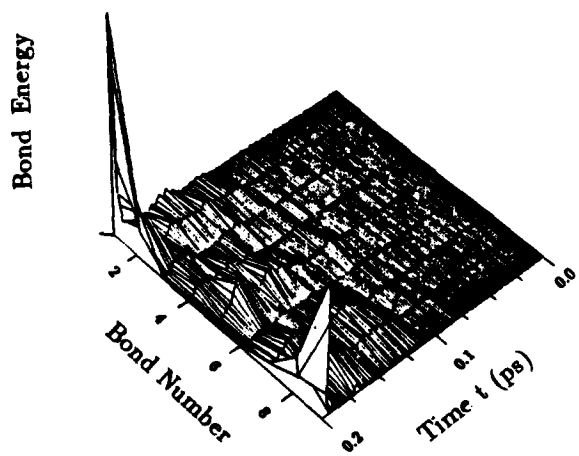

FIG. 19. The optimal field, power spectrum, and the bond energies for the combination ($\mu_1 = 7.5$ amu, $k_1 = 1.725$ a.u.). The local excitation is less successfully achieved in comparison to that in Fig. 18.

mining whether selective excitation can be achieved. Further optimal control calculations will be needed to fully assess this matter.

V. ROBUSTNESS ANALYSIS

From the above case studies one sees that the resultant optimal fields are complicated. Projecting ahead to the ultimate goal of laboratory field generation and applications the significance of field errors must be evaluated. Therefore, the question of sensitivity of bond energy to errors in the optimal pumping field naturally arises. In this section we will discuss this problem for harmonic chain molecules. For more realistic molecules further complications will arise necessitating the use of formal sensitivity analysis techniques.[12]

The solution to the Eq. (2.6) with the initial condition $\mathbf{z}(0) = \mathbf{0}$ can be expressed as

$$\mathbf{z}(t) = \int_0^t dt'\, \epsilon(t') \exp[\mathbf{A}(t-t')]\mathbf{b}. \tag{5.1}$$

Now suppose that the laboratory-generated field $\epsilon(t)$ has a random error $\Delta\epsilon(t)$ around the nominal field $\epsilon_0(t)$, where the latter field is given by the optimal control calculation, such that

$$\bar{\epsilon}(t') = \overline{\epsilon_0(t') + \Delta\epsilon(t')} = \epsilon_0(t'). \tag{5.2}$$

The overbar denotes an average over a large number of samples (experiments), since realistic laboratory results would be obtained with a large number of repeated pulse operations. Then the average value $\bar{\mathbf{z}}(t)$ of the observables over a large number of experiments is given by

$$\bar{\mathbf{z}} = \int_0^t dt'\, \epsilon_0(t') \exp[\mathbf{A}(t-t')]\mathbf{b} \tag{5.3}$$

and the deviation in $\mathbf{z}(t)$ due to the error $\Delta\epsilon(t')$ reads

$$\Delta\mathbf{z}(t) = \mathbf{z}(t) - \bar{\mathbf{z}}(t) = \int_0^t dt'\, \Delta\epsilon(t) \exp[\mathbf{A}(t-t')]\mathbf{b}. \tag{5.4}$$

Using Eqs. (2.8), (2.9), and (5.4), one can write the average deviation of the molecular energy at time T caused by $\Delta\epsilon(t)$ as

$$\begin{aligned}
\Delta\bar{E}_m &= \tfrac{1}{2}\,\overline{[\mathbf{z}^T(T)\mathbf{M}\mathbf{z}(T) - \bar{\mathbf{z}}(T)\mathbf{M}\bar{\mathbf{z}}(T)]} \\
&= \tfrac{1}{2}\,\overline{[\mathbf{z}^T(T) - \bar{\mathbf{z}}^T(T)]\mathbf{M}[\mathbf{z}(T) - \bar{\mathbf{z}}(T)]} \\
&= \frac{1}{2}\int_0^T dt' \int_0^T dt''\, \mathbf{b}^T\{\exp[\mathbf{A}^T(T-t')] \\
&\quad \times \mathbf{M}\exp[\mathbf{A}(T-t'')]\mathbf{b}\}\,\overline{\Delta\epsilon(t')\Delta\epsilon(t'')} \\
&= \frac{1}{2}\tau\int_0^T dt'\, f(t')\mathbf{b}^T\exp[\mathbf{A}^T(T-t')] \\
&\quad \times \mathbf{M}\exp[\mathbf{A}(T-t')]\mathbf{b},
\end{aligned} \tag{5.5}$$

where for simplicity we have assumed that

$$\overline{\Delta\epsilon(t')\Delta\epsilon(t'')} = \begin{cases} f(t') & \text{if } -\tau/2 \leqslant (t''-t') \leqslant \tau/2 \\ 0 & \text{otherwise} \end{cases} \tag{5.6a}$$

with τ being the error correlation time which is assumed sufficiently small such that the approximation

$$\int_{t'-\tau/2}^{t'+\tau/2} \exp[\mathbf{A}(T-t'')]dt'' \simeq \tau \exp[\mathbf{A}(T-t')] \tag{5.6b}$$

is valid. Similarly, the average deviation of the target ith bond energy at time T has the expression

$$\Delta\bar{e}_i = \frac{1}{2}\tau \int_0^T dt' f(t')\{\exp[\mathbf{A}(T-t')]\mathbf{b}\}_i^2 k_i + \{\exp[\mathbf{A}(T-t')]\mathbf{b}\}_{i+N}^2 G_{ii}, \tag{5.7}$$

where $\{\ \}_i$ denotes the ith component. Now we consider two kinds of error $f(t)$: the first one corresponds to a case of constant background noise and for the second case $f(t)$ is proportional to the field intensity itself. That is, we assume

$$f(t) = \begin{cases} \epsilon_b^2 & \text{for the first case} \\ C\epsilon_0^2(t) & \text{for the second case} \end{cases}, \tag{5.8}$$

where C is a proportionality constant. Substituting Eq. (5.8) into Eqs. (5.6) and (5.7) gives

$$\Delta\bar{E}_m(t) = \begin{cases} \frac{\tau}{2}\epsilon_b^2 \int_0^T \mathbf{b}^T \exp[\mathbf{A}^T(T-t')]\mathbf{M}\exp[\mathbf{A}(T-t')]\mathbf{b} & \text{for the first case,} \\ \frac{\tau}{2} C \int_0^T dt' \epsilon_0^2(t')\mathbf{b}^T \exp[\mathbf{A}^T(T-t')]\mathbf{M}\exp[\mathbf{A}(T-t')]\mathbf{b}, & \text{for the second case.} \end{cases} \tag{5.9}$$

and

$$\Delta\bar{e}_i = \begin{cases} \frac{\tau}{2}\epsilon_b^2 \int_0^T dt'\{\exp[\mathbf{A}(T-t')]\mathbf{b}\}_i^2 k_i + \{\exp[\mathbf{A}(T-t')]\mathbf{b}\}_{i+N}^2 G_{ii}, & \text{for the first case,} \\ \frac{\tau\epsilon}{2} \int_0^T dt'\{\epsilon_0(t')\exp[\mathbf{A}(T-t')]\mathbf{b}\}_i^2 k_i + \{\epsilon_0(t')\exp[\mathbf{A}(T-t')]\mathbf{b}\}_{i+N}^2 G_{ii} & \text{for the second case.} \end{cases} \tag{5.10}$$

Equations (5.9) and (5.10) state that the average deviations of the total molecular and the target bond energies are proportional to the error correlation time τ. As a reasonable value, we take τ to be equal to the grid step size of the discretized field in the following numerical calculations for illustration (i) in Sec. IV. We define $\Delta\bar{E}_m/E_m(T)$ and $\Delta\bar{e}_i/e_i(T)$ as the relative errors of the total molecular system and the target bond energies caused by the field error, respectively. Figure 20 shows the relative errors of the total molecular system and the target bond energies as functions of the time interval T for the case of constant background noise with $(\epsilon_b/\epsilon_p)^2 = 10^{-3}$ and ϵ_p being the peak value of the pulse pumping field. It is seen that the relative errors almost linearly increase with the increase of the time interval T for $T > 0.1$ ps. This behavior is understandable because the final energies $E_m(T)$ and $e_i(T)$ are independent of the time interval T while the average deviations of the energies $\Delta\bar{E}_m(T)$ and $\bar{e}_i(T)$ increase monotonically due to the posi-

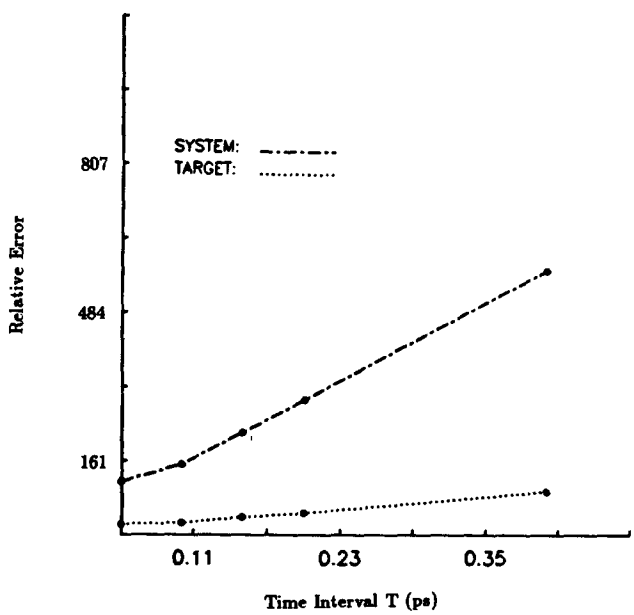

FIG. 20. The relative error of the total molecular system and the target bond energies as functions of the time interval T for the first kind of error in Eq. (5.8), the constant background noise, with $(\epsilon_b/\epsilon_p)^2 = 10^{-3}$.

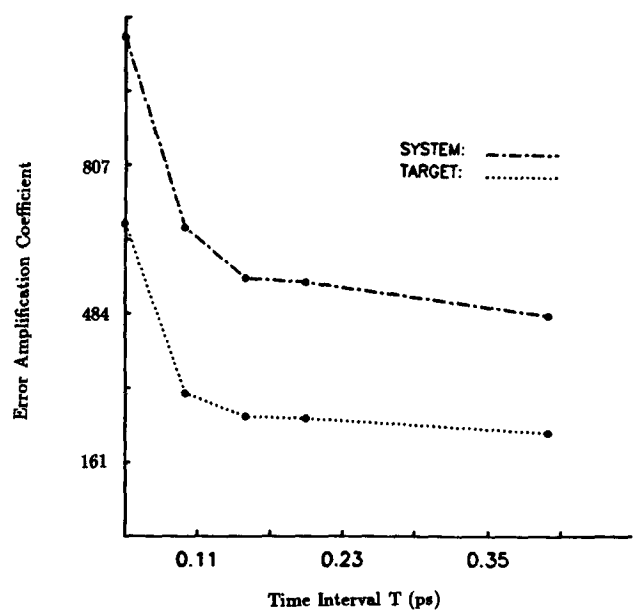

FIG. 21. The error amplification coefficients for the total molecular system and the target bond energies as functions of the time interval T for the second kind of error in Eq. (5.8).

tive nature of the integrands in Eqs. (5.9) and (5.10) for an error of the constant background noise. Physically the relative error increases with T since eventually the field error $f(t)$ will exceed $\epsilon_0^2(t)$ in the low amplitude region before the intense portion of the pulse.

The ratio of the relative errors to the error proportionality constant C for the second kind of error, which we call the error amplification coefficients are plotted in Fig. 21 as functions of the time interval T. In contrast with the case of constant background noise, in this case the error amplification coefficients first decrease rapidly for T up to ~ 0.1 ps, and then gradually approach their asymptotic values, respectively. This kind of behavior is a manifestation of the characteristic properties of the optimal fields described in Sec. IV. For $T < 0.1$ ps, the intensity of the optimal field decreases rapidly with increases in the time interval T. However, for $T > 0.1$ ps, the significant optimal field intensity as a function of $(T-t)$ becomes independent of T, and increasing T only lengthens the first period of the field when the intensity is very low and gradually approaches zero. Consequently, the average deviations $\Delta\bar{E}_m$ and $\Delta\bar{e}_i$ gradually become constant with increasing T. It should be pointed out that for the present choice of the error correlation time τ (equal to the grid size Δt in descretizing the time t) the relative errors as well as the amplification coefficients are quite large. Other choices of τ could lead to reduced errors.

VI. CONCLUDING REMARKS

In this work we have demonstrated how optimal control theory can be used to design an optical field for achieving a certain objective, say, selective local bond excitation. To begin with, one has to first set up an objective functional which is a mathematical transcription of the physical objectives. It will generally be beneficial to build in as much physical insight as possible into the objective functional. It is seen that the optimal fields, which lead to successfully achieved objectives, are complicated. Although with hindsight one can sometimes explain the gross features in the field, the complex structure makes it impossible to rely on spectral information alone to deduce the optimal optical field needed to selectively excite a local bond in a polyatomic molecule. This observation explains why previous laboratory attempts at bond selective chemistry have been discouraging. The apparent problem of quenching by rapid intramolecular energy transfer can be overcome by fields with specially designed structure that naturally results from applying the optimal control algorithm. The optimal fields depend on the choice of the weight factors $\mathbf{w}$ and w_e in the cost function L and the value of Q_s in the error function $\Phi(T)$. The underlying physical objectives dictate the choice of the weight factors which in turn determine the magnitude of the error function $\Phi(T)$. Larger weight factors will lead to larger value for the error function $\Phi(T)$. However, one always can make the final target bond stretch $\langle q(T)\rangle$ larger than a specified value by increasing the value Q_s.

It should be emphasized that the intention of the present work is to illustrate the applicability of optimal control theory in controlling molecular dynamics. The cases studied here are certainly over simplified model systems. To more realistically treat the problem one first has to take into account the anharmonicity which causes no fundamental difficulties, but leads to a much more complicated formalism and computational procedure.[9,13] Secondly, a host of other issues and effects need to be included. For example, molecular rotation needs to be incorporated and an assessment made of the sensitivity to molecular Hamiltonian and dipole function uncertainty. Furthermore, it is seen that for all the cases studied in this work due peak intensity of the resultant optimal field is very high. At such a high intensity, if the molecules are not ionized, at least the dipole will no longer be as independent of the optical field as we have assumed throughout this work. In principle, one could take this effect into account by including the electronic motion or by considering the polarizability of the molecule as a function of the optical field. Another alternative is to restrict the field intensity below a certain limit so that the dipole will be approximately independent of the optical field. Among other things, this intensity restricted optimal control will be discussed in another following paper.[14] In general, other pragmatic laboratory motivated restrictions might also be imposed on the field (e.g., a prescribed and modulated pulse shape envelope with control parameters to be determined).

Here we have been only concerned with selective vibrational excitations as our objectives. Actually, a similar approach can be used to develop the formalism for the design of the optical fields needed for controlling any kind of physical observables as objectives.[9] For example, a selective unimolecular chemical reaction can also be treated within the framework of the present optimal control algorithm which is different from the approaches proposed by Tannor and Rice,[4] Shapiro and Brumer,[5] and Holme and Hutchinson.[6] Shapiro and Brumer have treated a special case where a prepared state, which is a linear superposition of two nondegenerate bond eigenstates, is pumped into degenerate dissociative product states by two lasers. In this case there is a simple relation between the selectivity to one of the product states and the phases and amplitude effects due to both the superposition state preparation and subsequent applied fields. However, they have not presented a systematic procedure for a general reactive system where such a simple relation does not exist. Holme and Hutchinson have suggested using two or more lasers to coherently excite the molecule to nearly degenerate molecular eigenstates and to eliminate a unwanted zero order state by destructive interference. Again, their suggestion is feasible in principle only if the resultant projection onto the zero order state depends on the pumping fields in a simple form. In Tannor and Rice's scheme a sequence of two laser pulses are used. The first pulse excites the molecule into a nonstationary state on an excited electronic surface, which then evolves *freely* on that surface. The second pulse is variationally determined so as to stimulate deexcitation into a selected product channel on the ground electronic surface. In contrast, in our approach we would aim to design a field to optimize the *entire* dynamical process for reactive selectivity.

One topic that we have not mentioned in this work is the controllability of the problem (i.e., the ability to access an arbitrary state from any other system state in finite time). There are a number of works[13,15–17] that have been con-

cerned with this and related issues. As we pointed out above, the design of the optical field to achieve a specified objective is an inverse dynamical problem. To exactly solve this problem is a formidable task. Fortunately, in most cases such as the examples studied in the present work, the physical objectives are soft in the sense that it is sufficient to control the system as "best we can." That is, we only need to obtain an optimal solution to the inverse problem. The actual application of controllability concepts to these problems awaits further investigation.

Notwithstanding the idealized model illustrations in this work, it should be pointed out that the resultant optimal fields are short and intensive pulses which are too complicated in structure to be generated in the laboratory for the time being. The deviations from the desired objectives caused by the errors in the optical fields are independent of the fields themselves for the harmonic systems. In more general circumstances, the deviations would depend on the field itself. In that case, it is certainly desirable to build robustness criteria into the optical field design so that the physical observables could be achieved with the least sensitivity to the inevitable errors in generating the designed pumping field. This same type of robustness will likely be necessary with regard to molecular Hamiltonian and dipole function uncertainty.[12] This issue, as well as others, might be more easily dealt with in the incoherent optimal control regime, rather than in the coherent collision free context of the present paper.

The encouraging results of the present work clearly show the applicability of optimal control theory to the control of molecular dynamics. Although it is too premature to draw positive conclusions, it does seem promising that polyatomic molecules may be made to "dance" to *our* tunes.

ACKNOWLEDGMENTS

The authors acknowledge support for this work from the Office of Naval Research and the Air Force office of Scientific Research. We are grateful to Dr.A. Peirce for offering the modified conjugate gradient subroutine and to Dr. Hans Beumee for helpful suggestions, and would like to thank Professor M. Littman and Professor P. J. Ramadge for useful discussion on the topic of control theory.

[1]A. H. Zewail and N. Bloembergen, J. Phys. Chem. **88**, 5459 (1984).
[2]Aa. S. Sudbø, P. A. Schulz, E. R. Grant, Y. R. Shen, and Y. T. Lee, J. Chem. Phys. **70**, 912 (1979).
[3]J. M. Jasinski, J. K. Frisoli, and C. B. Moore, Faraday Discuss. Chem. Soc. **75**, 289 (1983).
[4](a) D. J. Tannor and S. A. Rice, J. Chem. Phys. **83**, 5013 (1985); Adv. Chem. Phys. **70** (1987); (b) S. A. Rice and D. J. Tannor, J. Chem. Soc. Faraday Trans. 2 **82**, 2423 (1986).
[5]M. Shapiro and P. Brumer, J. Chem. Phys. **84**, 4103 (1986); P. Brumer and M. Shapiro, Chem. Phys. Lett. **126**, 54 (1986).
[6]T. A. Holme and J. S. Hutchinson, Chem. Phys. Lett. **124**, 181 (1986); J. Chem. Phys. **86**, 42 (1987).
[7]S. Conolly, D. Nishimura, and A. Maeovski, IEEE Med. Im. **5**, 106 (1986).
[8]See, for example, D. G. Luenberger, *Introduction to Dynamic System, Theory, Models, and Applications* (Wiley, New York, 1979).
[9]S. Shi and H. Rabitz (to be published).
[10]See, for example, D. G. Luenberger, *Introduction to Linear and Nonlinear Programming* (Addison-Wesley, Reading, MA, 1973).
[11]J. Lewins, *Importance: the Adjoint Function* (Pergamon, New York, 1965).
[12]H. Rabitz, Chem. Rev. **87**, 101 (1987).
[13]A. Peirce and H. Rabitz, Phys. Rev. A (in press).
[14]S. Shi and H. Rabitz (to be published).
[15]A. G. Butkovskii and Y. I. Samoilenko, Auto. Rem. Control **A**, 485 (1979).
[16]A. G. Butkovskii and Y. Y. Samoilenko, Dokl. Akad. Nauk, SSSR **250**, 51 (1980).
[17]G. M. Huang, J. J. Tarn, and J. W. Clark, J. Math. Phys. **24**, 2608 (1983).